

Differential Expression of IR-A, IR-B and IGF-1R in Endometrial Physiology and Distinct Signature in Adenocarcinoma

Clare A. Flannery, Farrah L. Saleh, Gina H. Choe, Daryl J. Selen, Pinar H. Kodaman, Harvey J. Kliman, Teresa L. Wood, and Hugh S. Taylor

Obstetrics, Gynecology, and Reproductive Sciences (C.A.F., F.L.S., G.H.C., D.J.S., P.H.K., H.J.K., H.S.T.), Yale School of Medicine, New Haven, Connecticut 06520; Internal Medicine (C.A.F.), Yale School of Medicine, New Haven, Connecticut 06520; and Pharmacology, Physiology and Neuroscience and Cancer Center (T.L.W.), NJ Medical School, Rutgers University, Newark, New Jersey 07101

Context: Type 2 diabetes and obesity are risk factors for endometrial hyperplasia and cancer, suggesting that hyperinsulinemia contributes to pathogenesis. Insulin action through insulin receptor (IR) splice variants IR-A and IR-B regulates cellular mitogenesis and metabolism, respectively.

Objective: We hypothesized that IR-A and IR-B are differentially regulated in normal endometrium, according to mitogenic and metabolic requirements through the menstrual cycle, as well as in endometrial hyperplasia and cancer.

Design: IR-A, IR-B, and IGF-1 receptor (IGF-1R) mRNA was quantified in endometrium, endometrial epithelial and stromal cells, and in vitro after hormone stimulation.

Setting: Academic center.

Patients: Endometrium was collected from women with regular cycles ($n = 71$), complex hyperplasia ($n = 5$), or endometrioid adenocarcinoma ($n = 11$).

Intervention(s): In vitro sex-steroid treatment.

Main Outcome Measure(s): IR-A and IR-B expression

Results: IR-A increased dramatically during the early proliferative phase, 20-fold more than IR-B. In early secretory phase, IR-B and IGF-1R expression increased, reaching maximal expression, whereas IR-A decreased. In adenocarcinoma, IR-B and IGF-1R expression was 5- to 6-fold higher than normal endometrium, whereas IR-A expression was similar to IR-B. Receptor expression was unrelated to body mass index.

Conclusion: IR-A was elevated during the normal proliferative phase, and in endometrial hyperplasia and adenocarcinoma. The dramatic early rise of IR-A in normal endometrium indicates IR-A is the predominant isoform responsible for initial estrogen-independent endometrial proliferation as well as that of cancer. IR-B is elevated during the normal secretory phase when glucose uptake and glycogen synthesis support embryo development. Differing from other cancers, IR-B expression equals mitogenic IR-A in endometrial adenocarcinoma. Differential IR isoform expression suggests a distinct role for each in endometrial physiology and cancer. (*J Clin Endocrinol Metab* 101: 2883–2891, 2016)

Type 2 diabetes mellitus and obesity are risk factors for the development of endometrial hyperplasia and type 1 endometrioid adenocarcinoma in women (1–3). Exercise, weight loss, or metformin therapy are successful in reducing cancer risk as well as treating endometrial hyperplasia (4–6). Notably, most women with endometrial hyperplasia and adenocarcinoma are postmenopausal, with low or negligible serum levels of estradiol (E_2) (7–9). This epidemiological data suggests that other, nonestrogenic factors which are elevated with age, obesity, and insulin resistance, contribute to pathogenesis of endometrial hyperplasia and adenocarcinoma. In these settings, circulating insulin levels are elevated and may induce dysregulation of normal endometrial physiology, promoting abnormal proliferation and thereby predisposing to mutation.

The role of insulin in endometrial physiology is poorly characterized. Insulin is a mitogenic and metabolic hormone, and the endometrium requires coordinated regulation of intense mitogenic stimulus and carbohydrate metabolism to undergo critical structural and functional changes during a normal 28-day cycle. The first half of the menstrual cycle, the proliferative phase, involves simultaneous sloughing and repair of endometrial tissue, then rapid glandular proliferation (10). Tissue repair and early epithelial expansion occur independently of E_2 (11), but E_2 drives later glandular proliferation to a final thickness of approximately 10 mm (12). During the secretory phase, under the influence of progesterone (P_4), stromal cells proliferate, and both epithelial and stromal cells differentiate to prepare for embryo implantation and support through placentation. The glands synthesize glycogen, and secrete carbohydrate, adhesion molecules and immune-modulating chemokines, to attract and nourish an implanting embryo (13). If implantation does not occur, the cycle repeats. Insulin may work in concert with E_2 and P_4 to enable this sequence of cellular repair, proliferation, differentiation, and metabolism.

The cellular action of insulin is determined in part by the relative abundance and distribution of insulin receptor (IR) isoforms, IR-A and IR-B. The 2 isoforms are derived from alternative mRNA splicing of exon 11, which is present in IR-B and absent in IR-A (14, 15). Exon 11 encodes 12 amino acids present in the receptor's α -subunit (16). Insulin has higher binding affinity for IR-A than IR-B (16) and activates AKT, MAPK, and mTOR signaling through each receptor, although preferential activation of each pathway may differ (17, 18).

Activated IR-A promotes mitogenic activity in the cell (19–21). IR-A is the dominant isoform in fetal tissue and several cancers including breast, hepatocellular, lung, colon, and thyroid cancer (14, 22–25). Endogenous hyper-

insulinemia increases tumor growth in vivo (26). IR-B is the predominant isoform in liver and skeletal muscle (14, 22, 27), and in these tissues, insulin regulates metabolic cellular activity, including glucose uptake, glycogen synthesis, and lipid storage (18). IR-B is also involved in cell differentiation of adipocytes, hepatocytes, and hematopoietic cells (15). Because the relative distribution of IR-A and IR-B is tissue specific (14, 22, 27), alternative splicing is likely highly regulated to support functional differences in insulin action between tissues.

We hypothesized that insulin receptor isoforms IR-A and IR-B are differentially regulated during the menstrual cycle according to the mitogenic and metabolic needs of the endometrium. We hypothesized that IR-A is elevated during the proliferative phase in normal tissue, as well as in endometrial hyperplasia and adenocarcinoma. However, IR-B is elevated during the secretory phase when the epithelial cells differentiate into secretory glands and synthesize glycogen.

To study insulin's potential role in endometrial physiology, we characterized the distribution of IR-A and IR-B mRNA in normal endometrium across the menstrual cycle. At pathophysiological levels, insulin may also bind to the IGF-1 receptor (IGF-1R) (15). The IGF axis is well defined in endometrial physiology and implicated in endometrial cancer pathogenesis (28–30). We also quantified IGF-1R expression levels in normal and malignant endometrium. Endometrial hyperplasia is a spectrum of severity, thus we examined only complex hyperplasia, which is associated with a 30% transformation rate to endometrioid adenocarcinoma (31). Quantifying mRNA is the best modality to distinguish between these receptors due to the high homology among the proteins and unavailability of isoform-specific antibodies. Although IR isoform and IGF-1R levels or binding activity have been previously reported in several human tissues, the assays were not optimized to compare relative levels between these receptors (23, 32–34). Here, we use a highly specific quantitative real-time polymerase chain reaction (qRT-PCR) assay to quantify relative mRNA levels of IR-A, IR-B, and IGF-1R in human tissue with a focus on normal and pathological endometrium (35).

Materials and Methods

Endometrial adenocarcinoma, hyperplasia, and normal endometrium collection

The study of deidentified normal and pathological endometrium was approved by the Yale Human Investigations Committee. Written consent from patients was received by the Yale Gynecologic Oncology Tissue Bio-Repository for the collection of pathological endometrium and associated clinical data. Fresh

endometrial tissue was collected from healthy, reproductive age women undergoing elective gynecological surgery. Women who received exogenous hormonal therapy in the 3 months before tissue collection or had endometrial pathology were excluded. Clinical data included subject age, height, weight, last menstrual period or postmenopausal status, presence of type 2 diabetes, histological diagnosis, and cancer staging, as appropriate. Body mass index (BMI) was calculated and categorized per NIH criteria (36).

Normal tissue was processed immediately for one of 3 protocols. For total tissue analysis, tissues ($n = 45$) were collected into RNAlater (QIAGEN) and stored at -80°C . A portion of tissue was also collected in 10% nonbuffered formalin for histological endometrial dating by a gynecologic pathologist (37). For the *in vitro* hormone assay or analysis of cell-specific gene expression, tissue was collected and processed immediately with enzymatic digestion and cell type separation for RNA extraction ($n = 12$) or culture ($n = 14$).

For pathological tissue ($n = 16$), endometrium was collected into RNAlater at the time of histological frozen section within ten minutes of hysterectomy. A gynecologic pathologist diagnosed hyperplasia or adenocarcinoma by light microscopic examination of hematoxylin and eosin-stained slides, and tissue was collected immediately adjacent to the diagnostic specimen. Final histology was confirmed and classified per the World Health Organization (38). Surgical staging was per the International Federation of Gynecology and Obstetrics (39). Hyperplasia tissue included in this study ($n = 5$) was complex, with or without atypia. All cancer tissue ($n = 11$) was type 1 endometrioid adenocarcinoma, with or without squamous differentiation.

Immunohistochemistry

Endometrial tissue was fixed in formalin, embedded in paraffin, cut into $5\text{-}\mu\text{m}$ sections, and mounted onto charged slides. Slides were deparaffinized and dehydrated through a series of xylene and ethanol washes and immunohistochemically stained with Ki67 antibody (clone MIB-1; Dako North America) using EnVision+ System-HRP (diaminobenzidine) (Dako), as previously described (40). Normal mouse ascites (clone NS-1; Sigma-Aldrich) staining of each endometrial sample served as a negative control, and Ki67 staining of tonsil served as a positive control.

Primary cell isolation, culture, and *in vitro* assays

Epithelial and stromal cells were isolated from endometrial tissue, and evaluated separately, in experiments 1) to localize receptor expression in each cell type, and 2) to determine hormone regulation of receptor expression. Endometrial epithelial and stromal cells were isolated from normal endometrium as previously validated by immunocytochemical analyses (41, 42). Tissue was minced, then enzymatically digested using Collagenase B and DNase I in Hank's Balanced Salt Solution. Epithelial and stromal cells were separated using $40\text{-}\mu\text{m}$ mesh cell strainers (BD Falcon) and selective plating. To localize receptor expression in each phase of the menstrual cycle, isolated epithelial and stromal cells from endometrial tissue ($n = 12$) were immediately lysed, separately, and RNA was extracted from each lysate.

To evaluate the effect of E_2 and P_4 on receptor expression, primary epithelial and stromal cells isolated from endometrial tissue ($n = 14$) were cultured separately at 37°C in 5.5mM glucose DMEM (Life Technologies) with 10% fetal bovine serum, 1% penicillin/streptomycin, and 1% amphotericin B. Once confluent, cells were starved for 4 hours in serum-free, phenol-free 5.5mM glucose DMEM, then treated for 6 hours with 10nM E_2 , 1 μM P_4 , combined E_2 and P_4 , or 0.1% ethanol (vehicle). Cells were lysed, and RNA was extracted. P_4 receptor and heart and neural crest derivatives expressed transcript 2 (Hand2) mRNA levels were quantified as internal controls for *in vitro* experiments.

RNA extraction

Endometrial tissues and isolated endometrial cells were homogenized in TRIzol (Life Technologies). RNA was isolated with chloroform, precipitated with isopropanol, washed with 75% ethanol, and dissolved in RNase-free water. RNA was treated with RNase-free DNase and purified via RNeasy spin columns. For *in vitro* studies, RNA was extracted from cultured cells using RNeasy Mini kit (QIAGEN). RNA concentration and purity analysis was determined via Nanodrop 2000 (Thermo Scientific).

Human insulin receptor isoform and IGF-1R qRT-PCR primers and optimization

Highly specific primers for IR-A, IR-B, and IGF-1R mRNA were designed using Primer Premier v5 Software (Premier Biosoft

Table 1. Clinical Characteristics of Study Population

	Normal Endometrium	Complex Hyperplasia	<i>P</i> Value ^d	Endometrioid Adenocarcinoma	<i>P</i> Value ^d
<i>n</i>	45	5		11	
Age, y ^a	36 \pm 1	56 \pm 2	<.0001	60 \pm 4	<.0001
BMI, ^a kg/m ²	29.3 \pm 1.2	33.5 \pm 3.7	.3	37.5 \pm 3.0	.006
Normal ^b	19 (43.2%)	1 (20%)		0 (0.0%)	
Overweight ^b	8 (18.2%)	2 (40%)		1 (9.1%)	
Obese ^b	12 (27.3%)	0 (0%)		7 (63.6%)	
Extreme obesity ^b	5 (11.4%)	2 (40%)		3 (27.3%)	
Postmenopause ^c	0 (0.0%)	4 (80%)		10 (91%)	
T2DM ^c	0 (0.0%)	1 (20%)		3 (27.3%)	

^a Expressed as mean \pm SEM.

^b Expressed as *n* (%). BMI categories determined by NIH definitions.

^c Expressed as *n* (%).

^d Calculated by a Student's *t* test. Compared with normal endometrium.

International) to detect accurately all 3 receptors by qRT-PCR (35). To enable a direct comparison of relative receptor expression levels, a standard concentration curve of cDNA from each receptor, as synthesized via plasmids, was performed as previously described (35, 43). Detailed testing of assay specificity was performed using competition assays and postamplification analysis by gel electrophoresis and cloning (35). Primers for the P₄ receptor and Hand2 were designed via Primer Blast (<http://www.ncbi.nlm.nih.gov/tools/primer-blast>; NCBI, Bethesda, MD). Primers were synthesized at the W.M. Keck Foundation Oligo Synthesis Resource (Yale University, New Haven, CT). Optimal primer concentrations were determined by assessing

efficiency at different forward and reverse primer concentration combinations using 2-fold serial dilution of cDNA synthesized from human universal RNA (QIAGEN Sciences) (Supplemental Table 1) (35).

Reverse transcription and qRT-PCR analysis

For analysis of gene expression, qRT-PCR was performed using 12.5 ng of RNA reverse transcribed to cDNA, in duplicate or triplicate using assay-specific primer concentrations, SYBR Green containing dNTPs, fluorescein, and DNA polymerase (Bio-Rad), and amplified in a Bio-Rad CFX96 detection system (Bio-Rad) under the following cycling conditions: 95°C for 3 minutes, 40 cycles of 95°C for 15 seconds followed by 60°C for 30 seconds and 72°C for 25 seconds, 95°C for 1 minute, 55°C for one minute, and an increase to 95°C at 0.5°C increments.

Statistical analysis

Statistical differences for age and BMI within each cohort were analyzed via Student's 2-tailed *t* test. Gene expression obtained by qRT-PCR was normalized to β -actin and graphically represented as individual data points or as mean \pm SEM. Statistical significance for tissue experiments was determined by one-way ANOVA or Student's *t* test, using GraphPad Prism (GraphPad Software, Inc). Interreceptor comparisons and in vitro data were matched within tissue or per vehicle, respectively. Significance was defined as $P \leq .05$, after multiple-comparisons correction with Tukey's test. Receptor comparison between epithelial and stromal cells was determined by Wilcoxon matched pairs test, using GraphPad Prism.

Results

Patient characteristics

Endometrial tissue was collected from 45 reproductive-age women of mean age 36 ± 1 years with normal menstrual cycles, who were not receiving exogenous hormone therapy and had no endometrial pathologies (Table 1). Mean BMI was 29.3 ± 1.2 kg/m², with 61.4% of women being normal weight or overweight. None of these women had type 2 diabetes. Per endometrial dating, tissues were categorized as early proliferative (EP) ($n = 6$), late proliferative (LP) ($n = 21$), early secretory (ES) ($n = 8$), or late secretory (LS) ($n = 10$).

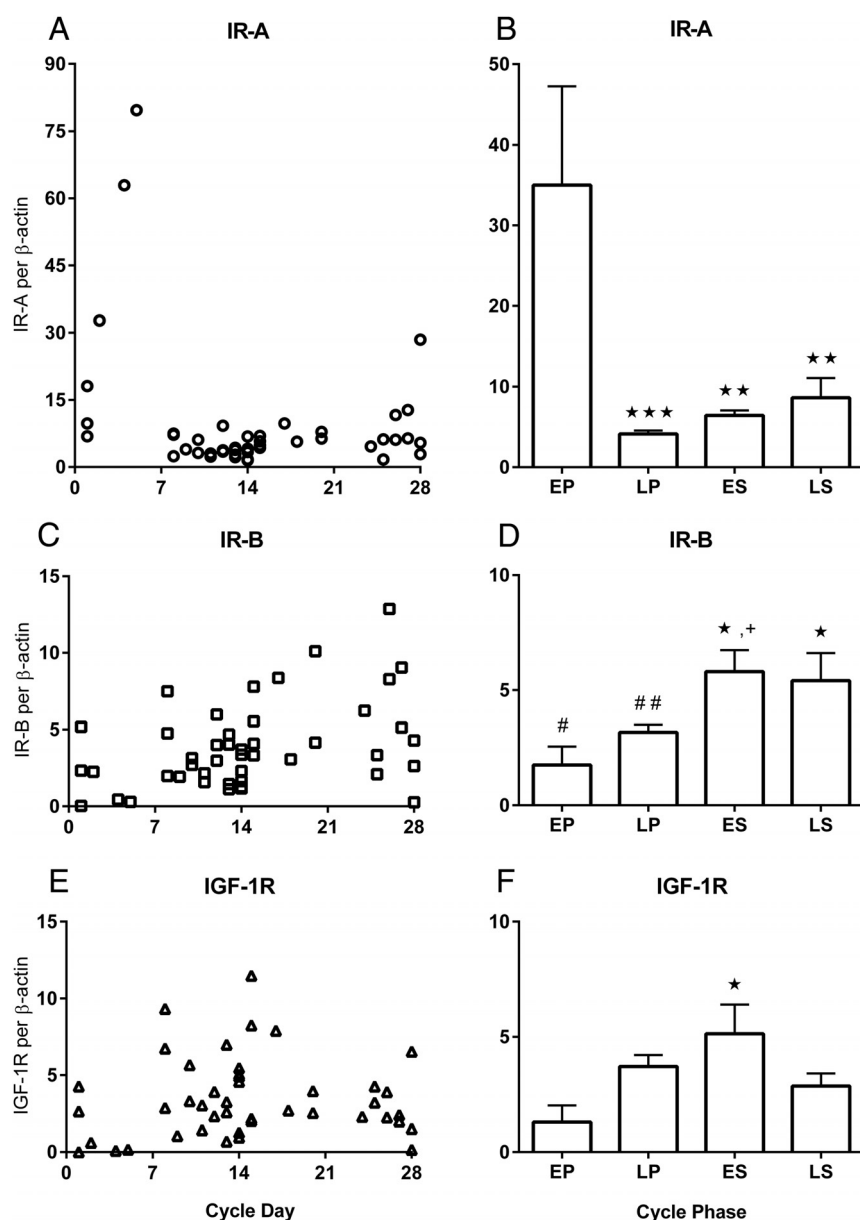


Figure 1. IR-A, IR-B, and IGF-1R mRNA levels across the menstrual cycle in normal endometrial tissue from 45 women. Graphs (A) IR-A (○), (C) IR-B (□), and (E) IGF-1R (Δ) show individual tissue levels by day of the menstrual cycle. Graphs (B) IR-A, (D) IR-B, and (F) IGF-1R are mean receptor levels \pm SEM for each phase of the menstrual cycle: EP (d 1–7), LP (d 8–14), ES (d 15–21), and LS (d 22–28). The y-axis for IR-A graphs are scaled differently due to higher levels in EP. The significance is defined as follows: *, $P \leq .05$ vs EP; **, $P \leq .01$ vs EP; ***, $P \leq .001$ vs EP; +, $P \leq .05$ vs LP; #, $P \leq .05$ vs IR-A; ## $P < .005$ vs IR-A.

Complex hyperplasia tissue was collected from 5 women of mean age 56 ± 2 years and mean BMI of 33.5 ± 3.7 kg/m² (Table 1). Four (80%) women were postmenopausal. Three women (60%) were normal weight or overweight. One (20%) woman had type 2 diabetes. On histology, nuclear atypia was present in 3 (60%) tissues. Type 1 endometrioid adenocarcinoma tissues were collected from 11 women of mean age 60 ± 4 years (Table 1). Ten (91%) women were postmenopausal. Mean BMI was 37.5 ± 3.0 kg/m², which was higher than the mean BMI of women with normal endometrium ($P = .006$). Ten (91%) of these woman were obese or morbidly obese. Three (27%) women had type 2 diabetes. For adenocarcinoma specimens, International Federation of Gynecology and Obstetrics staging (39) was stage IA (invasion to <50% of myometrium, $n = 5$); stage IB (invasion to >50% of myometrium, $n = 4$); or stage IIIC2 (including paraaortic lymph node involvement, $n = 2$). The clinical characteristics of these cohorts were consistent with known risk factors in women presenting with endometrial hyperplasia or adenocarcinoma, including age more than 50 years, postmenopausal status, obesity, and type 2 diabetes.

IR-A, IR-B, and IGF-1Rs are differentially expressed across the menstrual cycle

In normal endometrium, IR-A, IR-B, and IGF-1R were differentially expressed across the menstrual cycle (Figure 1). IR-A expression ascended dramatically in the first 5 days of the cycle (Figure 1A). Mean IR-A levels were highest in EP: 8.5-fold higher than LP ($P \leq .0001$), 5.4-fold higher than ES ($P \leq .001$), and 4-fold higher than LS ($P \leq .001$) (Figure 1B). Although IR-A levels were lowest in LP, mean IR-A increased gradually during the secretory phases. The increase in IR-A expression by the end of the cycle indicates the physiological continuum between days 28 and 1 of the menstrual cycle.

In contrast to the expression pattern of IR-A, IR-B levels were lowest in the EP phase and highest in the secretory phases (Figure 1C). Compared with the lowest levels in EP, mean IR-B levels were more than 3-fold higher in each of the secretory phases, ES and LS ($P \leq .05$) (Figure 1D). IR-B increased by 1.8-fold between LP and LS ($P \leq .05$). IR-B expression was similar between the secretory phases, ES and LS ($P =$ nonsignificant [NS]).

In the normal cycling endometrium, IGF-1R expression was also lowest in the EP phase, with highest levels in the ES phase (Figure 1E). Mean IGF-1R levels were 4-fold higher in ES than EP ($P \leq .05$) (Figure 1F).

The IR isoforms had a different pattern of expression across the menstrual cycle, with IR-A peaking in the EP phase and IR-B peaking in the secretory phases (Figure 1).

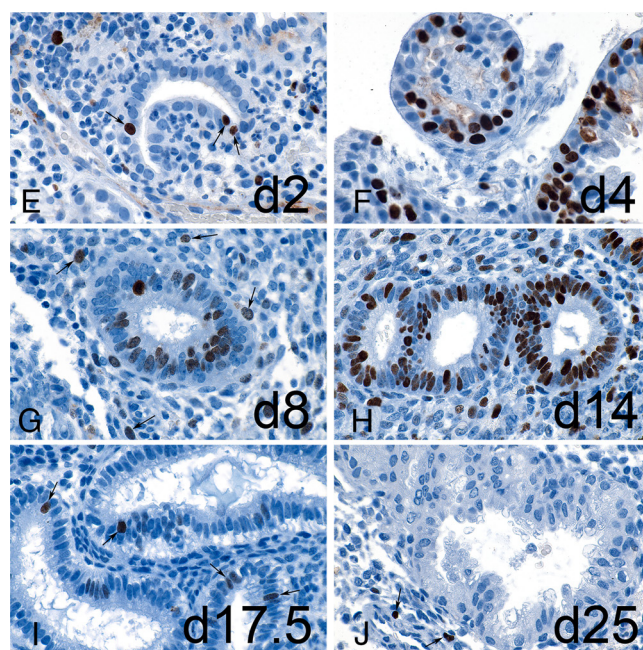
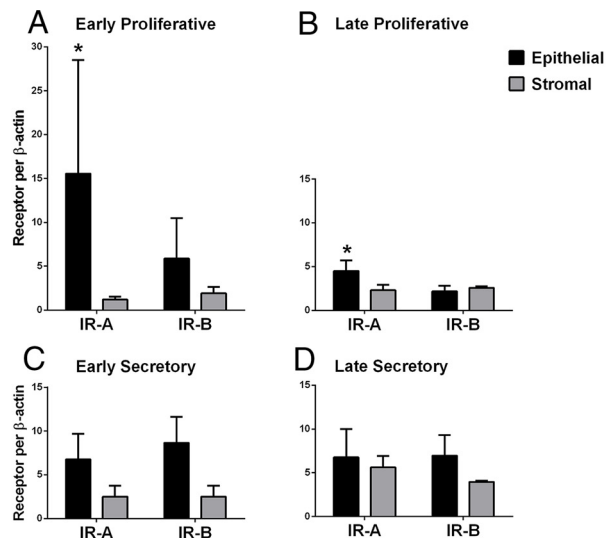


Figure 2. Distribution of IR-A and IR-B mRNA and Ki67 protein in endometrial epithelial and stromal cells. Mean IR-A and IR-B expression from each cell type isolated from normal endometrial tissues in EP (A), LP (B), ES (C), and LS (D) phases. *, $P \leq .03$, epithelial vs stromal. Ki67 immunohistochemistry of benign endometrium from cycle days 2 to 25, magnification $\times 900$. E, Cycle day 2 endometrium reveals mixture of menstrual debris and gland fragments, one of which has 3 Ki67 positive nuclei (arrows). F, Cycle day 4 endometrium showing glands with many darkly stained positive nuclei. G, Cycle day 8 endometrium with Ki67 positive glands and intact stroma, containing scattered Ki67 positive nuclei (arrows). H, Cycle day 14 endometrium exhibiting many Ki67 positive glands and stromal cells. I, Cycle day 17.5 endometrium reveals large glands with sub- and supranuclear vacuoles, and few Ki67 positive glandular nuclei (arrows). J, Cycle day 25 endometrium has complex glands without Ki67 positive nuclei; however, several stromal nuclei are Ki67 positive (arrows).

This qRT-PCR assay was optimized for interreceptor comparisons of IR-A and IR-B (35). Mean IR-A levels were 20-fold higher than IR-B in EP ($P \leq .05$), and 1.3-fold higher in LP ($P = .001$). Overall, the ratio of IR-A to IR-B was 20:1 in EP, 4:3 in LP, 1:1 in ES, and 3:2 in LS.

Epithelial and stromal cell expression of IR-A and IR-B

After finding differences in IR isoform expression during each phase of the menstrual cycle in total endometrial tissue, we sought to determine relative expression in epithelial and stromal cells. The IR-A and IR-B proteins differ by only 12 amino acids, and sensitive and specific antibodies to each receptor isoform are not available for either Western blotting or immunohistochemical localization. Hence, we extracted mRNA from epithelial and stromal cells isolated immediately from fresh endometrial tissues, separate from those used in the total tissue profile. IR-A and IR-B were present in both cell types in all phases of the menstrual cycle (Figure 2). Interestingly, the dramatic increase in IR-A during the proliferative phase occurred predominantly in the epithelial cells ($P = .03$, epithelial vs stromal) (Figure 2A).

Ki67 staining of endometrial glands

Gland formation occurs steadily during the proliferation phase, producing peak tissue thickness by midcycle. We stained endometrial tissues with proliferation marker Ki67 to demonstrate the normal physiology of the glands in relation to maximal IR-A and IR-B expression (Figure 2). Early gland formation is evident by day 2 with positive nuclear Ki67 staining in epithelial cells (Figure 2E), when IR-A begins to increase (Figure 1A). By day 4, epithelial proliferation is marked although the number of glands are still few (Figure 2F), when IR-A is reaching peak levels, predominantly in the epithelial cells (Figure 2A). By days 8 to 14 of the LP phase,

the number of glands increase substantially and stromal cells proliferate (Figure 2, G and H). At this time, IR-A expression is lowest in the endometrium, indicating that the dominant role of IR-A is already complete. By day 17 (Figure 2I), Ki67 staining in glands and stroma is minimal, and instead secretory vacuoles are visualized at the same time IR-B levels are peaking (Figure 2C). IR-B remains elevated through day 25, when Ki67 staining is absent in the epithelial nuclei and glandular structure is looser in the postimplantation window (Figure 2J).

E₂ and P₄ regulation of IR-A, IR-B, or IGF-1R in vitro

Because the receptors displayed a cyclical change in expression, we investigated whether the receptors are regulated by E₂ and P₄. In particular, we hypothesized that IR-B and IGF-1R are regulated by P₄, because their expression levels were highest in the secretory phase. The expression of IR-A, IR-B, or IGF-1R was unchanged in epithelial cells treated with E₂, P₄, or a combination of these hormones, relative to vehicle ($P = NS$) (Figure 3, A–C). As a positive control, P₄ receptor mRNA was increased in E₂-treated epithelial cells (data not shown). The lack of direct regulation of IR-A by E₂ in epithelial cells aligns with findings that IR-A's rapid increase in epithelial cells occurs during low serum E₂ levels in EP (9).

In stromal cells, the expression of IR-A was modestly increased 1.4-fold after E₂ treatment ($P \leq .01$) (Figure 3D). IR-B levels in stromal cells were not significantly altered by either E₂ or P₄ ($P = NS$) (Figure 3E). In response to P₄, IGF-1R expression was increased in stromal cells ($P \leq .05$) (Figure 3F), which is consistent with the rise in expression levels between LP and LS in noncultured stromal cells (Figure 2). As a positive control for P₄ response, Hand2 mRNA was found to be increased in P₄-treated stromal cells (data not shown).

No Effect of BMI on receptor expression

The mean BMI of the women with adenocarcinoma was higher than the mean BMI of women with normal endometrium. Therefore, we evaluated whether BMI influenced receptor expression in women with normal endometrium, of whom 38.7% were obese or morbidly obese. Neither IR-A nor IR-B correlated with BMI ($R = 0.08$ and $R = 0.18$, re-

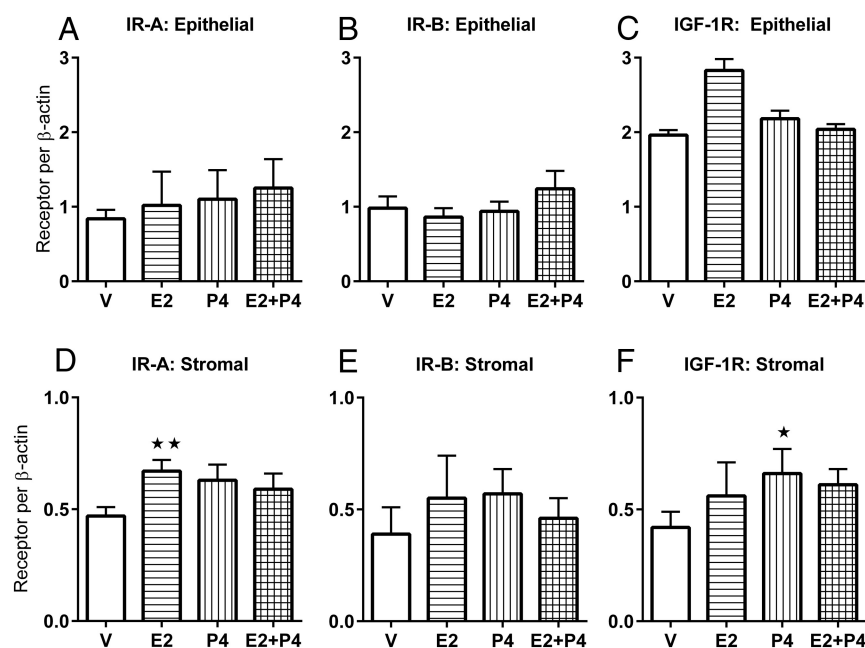


Figure 3. In vitro hormone assay to determine whether IR-A, IR-B, and IGF-1R are regulated by E₂ and/or P₄. Isolated epithelial ($n = 4$) and stromal cells ($n = 5$) from endometrial tissues were treated separately for 6 hours with E₂ 10–8M (E), P₄ 10–6M (P), combined E + P, or vehicle (V). Mean \pm SEM mRNA levels are shown for epithelial cell IR-A (A), IR-B (B), IGF-1R (C), and stromal cell IR-A (D), IR-B (E), and IGF-1R (F). *, $P \leq .05$ vs V; **, $P \leq .01$ vs V.

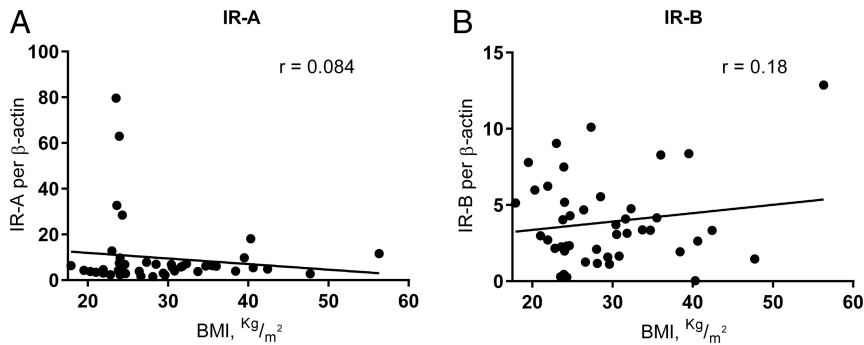


Figure 4. IR-A (A) and IR-B (B) levels from normal endometrial tissue do not correlate with BMI.

spectively) (Figure 4, A and B). IGF-1R also did not correlate with BMI ($R = 0.23$) (data not shown).

IR-A, IR-B, and IGF-1R expression in malignant and premalignant endometrium

IR-A, IR-B, and IGF-1R, were elevated in complex hyperplasia and endometrioid adenocarcinoma compared with normal proliferative endometrial tissue, excluding comparison of IR-A in the EP phase when IR-A had dramatic elevations. In endometrial complex hyperplasia tissues, mean IR-A expression trended lower than EP but was 3-fold higher than LP ($P \leq .01$) (Figure 5A). Surprisingly, IR-B expression in endometrial hyperplasia was higher than in any phase of normal endometrium, including 9-fold higher than EP ($P \leq .001$) and 5.2-fold higher than LP ($P \leq .0001$) (Figure 5B). Notably, IR-B expression was higher in hyperplasia than in adenocarcinoma ($P \leq .05$). IGF-1R expression in endometrial hyperplasia was also elevated compared with normal proliferative endometrium, specifically 9.9-fold higher than EP ($P \leq .0001$) and 3.4-fold higher than LP ($P \leq .001$) (Figure 5C).

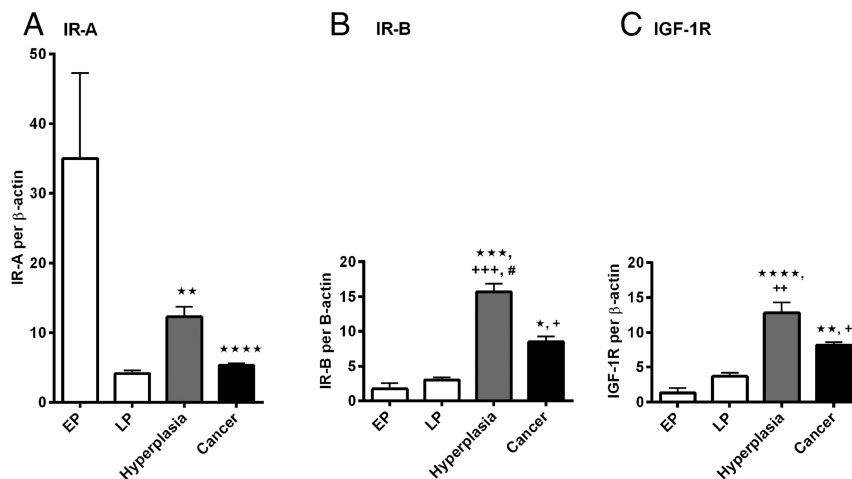


Figure 5. Mean mRNA levels \pm SEM of IR-A (A), IR-B (B), IGF-1R (C) in complex hyperplasia ($n = 5$) and type 1 endometrioid adenocarcinoma ($n = 11$), as compared with normal endometrial tissue in the EP and LP phases previously represented in Figure 2. The significance is defined as follows: *, $P \leq .05$ vs EP; **, $P \leq .01$ vs EP; ***, $P \leq .001$ vs EP; ****, $P \leq .0001$ vs EP; +, $P \leq .05$ vs LP; ++, $P \leq .001$ vs LP; +++, $P \leq .0001$ vs LP; #, $P \leq .05$ vs adenocarcinoma.

In type 1 endometrioid adenocarcinoma, mean IR-A expression was 84.8% lower than EP ($P \leq .0001$), but was similar to LP ($P = \text{NS}$) (Figure 5A). IR-B expression was 4.9- and 2.7-fold higher in adenocarcinoma than EP ($P \leq .05$) and LP ($P \leq .05$) (Figure 5B). IGF1-R expression in adenocarcinoma was 6.3- and 2.2-fold higher than EP ($P \leq .01$) and LP ($P \leq .05$) (Figure 5C).

Mean IR-A and IR-B levels were similar in complex hyperplasia ($P = \text{NS}$), as well as adenocarcinoma ($P = \text{NS}$) (Figure 5). Hence, no receptor isoform was dominant in the premalignant and malignant tissue. Expression of both IR-A and IR-B were significantly different than in benign endometrium.

Discussion

In this study, we characterized the differential expression of IR-A, IR-B, and IGF-1R in the endometrium. We found that IR-A was the most abundant receptor during the EP phase, when a rapid and dramatic increase in expression occurred predominantly in epithelial cells. High epithelial expression occurring this early in the cycle strongly indicates that activated IR-A may regulate initial epithelial proliferation and repair of glandular surfaces in the setting of menstruation. The formation of a new luminal epithelium occurs between days 2 and 6 of the menstrual cycle (44). Importantly, endometrial repair occurs when E_2 levels are very low (9) and is shown to be an estrogen-independent process (11). Accordingly, our findings show E_2 did not regulate IR-A expression in epithelial cells in vitro. For women with hyperinsulinemia, the presence of an insulin receptor, which may promote epithelial proliferation, independently of estrogen, is concerning.

In our cohort, most women with hyperplasia or adenocarcinoma were postmenopausal and obese, with 25% having type 2 diabetes, which is consistent with disease epidemiology (7). IR-A levels were not influenced by BMI in normal endometrium, yet remained high in hyperplasia and adenocarcinoma. Not surprisingly, IR-A was higher in the EP phase than in hyperplasia or adenocarcinoma

because normal endometrial glands proliferate to create a thick layer of 10 mm in less than 2 weeks (12), whereas hyperplasia and endometrioid adenocarcinoma progress over months to years (7).

In contrast to IR-A expression patterns, IR-B reached peak levels in the secretory phase. IR-B was more prominent in epithelial cells, indicating a role in epithelial differentiation into secretory cells during decidualization and in metabolism, when insulin activation of IR-B may regulate glycogenesis. An abundance of glycogen is synthesized rapidly in epithelial cells during the secretory phase, with an extrusion of carbohydrate material into the lumen, to be used as fuel for an implanted embryo (13). If pregnancy occurs, the glands provide the embryo with nutrition until approximately 8–10 weeks of gestation when the maternal-placental vascular system becomes functional (13). Similar to embryos, tumors have high metabolic requirements.

We found that IR-B was significantly elevated in complex hyperplasia and adenocarcinoma, relative to normal tissue. Because we found higher levels of IR-A than IR-B in normal proliferative tissue but similar levels in hyperplasia and adenocarcinoma tissue, abnormally proliferating endometrial cancer cells may selectively enhance inclusion of exon 11 during splicing of IR mRNA. This finding is in contrast to studies in breast, hepatocellular, lung, colon, and thyroid cancer, in which IR-A was the predominant isoform (22–25). Because the endometrium must maintain glycogenesis to supply embryonic needs independent of maternal diet, it is possible that the endometrium has the unique ability to maintain elevated levels of IR-B, and this normal physiology may be exploited by tumor cells.

Our findings that IGF-1R levels are highest in the secretory phase and P₄ stimulates increased IGF-1R expression is consistent with the physiological role of IGF-1 in decidualization, as preparation for blastocyst implantation (29), and align with previous reports (28). IGF-1R is known to have mitogenic capabilities, similar to IR-A. Surprisingly, IGF-1R expression was lowest during glandular mitogenesis in normal endometrium, suggesting IGF-1 is not a regulator of normal endometrial proliferation, a paradigm primarily supported by studies in mice (45, 46). However, IGF-1R was elevated in hyperplasia and adenocarcinoma over normal endometrium, indicating a pathogenic role in malignancy, consistent with previous reports (47).

In summary, we identified IR-A as highly regulated during the EP phase of the menstrual cycle. IR-A likely drives endometrial repair after menstruation and early epithelial proliferation, in the estrogen independent phase of the menstrual cycle. IR-B expression is prominent in the secretory phase when it likely promotes the metabolic

changes associated with embryo implantation. Elevated insulin levels may alter endometrial growth and function in fertility through both IR-A and IR-B. The role of IR-A in endometrial proliferation may be related to the increase in endometrial cancer seen in women with obesity and type 2 diabetes. Targeted IR-A or IR-B specific therapies may be useful in disorders of endometrial development including hyperplasia, cancer, and infertility.

Acknowledgments

We thank Pei Hui, MD, PhD, and Natalia Buza, MD, for reviewing endometrial hyperplasia and adenocarcinoma specimens at the time of frozen section; Michelle Montagna, MSc, and the Yale Gynecologic Oncology Bio-Repository for assistance in tissue collection; and Kristin Milano, BA, for her assistance with immunohistochemistry.

Address all correspondence and requests for reprints to: Clare A. Flannery, MD, Department of Obstetrics, Gynecology, and Reproductive Sciences, Yale School of Medicine, 333 Cedar Street, New Haven, CT 06520. E-mail: clare.flannery@yale.edu.

This work was supported by National Institutes of Health grants from the Eunice Kennedy Shriver National Institute of Child Health and Human Development K08HD071010 and U54 HD052668 (to C.A.F.).

Disclosure Summary: T.L.W. is an inventor on a patent application serial number 12/721,327 issued as a United States Patent 8377655 on 2/19/2013 “Assay for the Measurement of IGF type 1 Receptor and Insulin Receptor Expression.” C.A.F., F.L.S., G.H.C., D.J.S., P.H.K., H.J.K., and H.S.T. have nothing to disclose.

References

1. Friberg E, Orsini N, Mantzoros CS, Wolk A. Diabetes mellitus and risk of endometrial cancer: a meta-analysis. *Diabetologia*. 2007;50:1365–1374.
2. Reeves GK, Pirie K, Beral V, Green J, Spencer E, Bull D. Cancer incidence and mortality in relation to body mass index in the Million Women Study: cohort study. *BMJ*. 2007;335:1134.
3. Austin H, Austin JM Jr, Partridge EE, Hatch KD, Shingleton HM. Endometrial cancer, obesity, and body fat distribution. *Cancer Res*. 1991;51:568–572.
4. Patel AV, Feigelson HS, Talbot JT, et al. The role of body weight in the relationship between physical activity and endometrial cancer: results from a large cohort of US women. *Int J Cancer*. 2008;123:1877–1882.
5. Adams TD, Stroup AM, Gress RE, et al. Cancer incidence and mortality after gastric bypass surgery. *Obesity*. 2009;17:796–802.
6. Session DR, Kalli KR, Tummon IS, Damario MA, Dumesic DA. Treatment of atypical endometrial hyperplasia with an insulin-sensitizing agent. *Gynecol Endocrinol*. 2003;17:405–407.
7. Amant F, Moerman P, Neven P, Timmerman D, Van Limbergen E, Vergote I. Endometrial cancer. *Lancet*. 2005;366:491–505.
8. Potischman N, Hoover RN, Brinton LA, et al. Case-control study of endogenous steroid hormones and endometrial cancer. *J Natl Cancer Inst*. 1996;88:1127–1135.
9. Sherman BM, Korenman SG. Hormonal characteristics of the hu-

- man menstrual cycle throughout reproductive life. *J Clin Invest*. 1975;55:699.
10. Petracco RG, Kong A, Grechukhina O, Krikun G, Taylor HS. Global gene expression profiling of proliferative phase endometrium reveals distinct functional subdivisions. *Reprod Sci*. 2012;19:1138–1145.
 11. Kaitu'u-Lino TJ, Morison NB, Salamonsen LA. Estrogen is not essential for full endometrial restoration after breakdown: lessons from a mouse model. *Endocrinology*. 2007;148:5105–5111.
 12. Bromer JG, Aldad TS, Taylor HS. Defining the proliferative phase endometrial defect. *Fertil Steril*. 2009;91:698–704.
 13. Burton GJ, Watson AL, Hempstock J, Skepper JN, Jauniaux E. Uterine glands provide histiotrophic nutrition for the human fetus during the first trimester of pregnancy. *J Clin Endocrinol Metab*. 2002;87:2954–2959.
 14. Seino S, Bell GI. Alternative splicing of human insulin receptor messenger RNA. *Biochem Biophys Res Commun*. 1989;159:312–316.
 15. Belfiore A, Frasca F, Pandini G, Sciacca L, Vigneri R. Insulin receptor isoforms and insulin receptor/insulin-like growth factor receptor hybrids in physiology and disease. *Endocr Rev*. 2009;30:586–623.
 16. Mosthaf L, Grako K, Dull T, Coussens L, Ullrich A, McClain D. Functionally distinct insulin receptors generated by tissue-specific alternative splicing. *EMBO J*. 1990;9:2409.
 17. Leibiger B, Leibiger IB, Moede T, et al. Selective insulin signaling through A and B insulin receptors regulates transcription of insulin and glucokinase genes in pancreatic β cells. *Mol Cell*. 2001;7:559–570.
 18. Nystrom FH, Quon MJ. Insulin signalling: metabolic pathways and mechanisms for specificity. *Cell Signal*. 1999;11:563–574.
 19. Massagué J, Blinderman LA, Czech MP. The high affinity insulin receptor mediates growth stimulation in rat hepatoma cells. *J Biol Chem*. 1982;257:13958–13963.
 20. Gómez-Hernández A, Escribano Ó, Perdomo L, et al. Implication of insulin receptor A isoform and IRA/IGF-IR hybrid receptors in the aortic vascular smooth muscle cell proliferation: role of TNF- α and IGF-II. *Endocrinology*. 2013;154:2352–2364.
 21. Bonnesen C, Nelander GM, Hansen BF, et al. Synchronization in G0/G1 enhances the mitogenic response of cells overexpressing the human insulin receptor A isoform to insulin. *Cell Biol Toxicol*. 2010;26:293–307.
 22. Frasca F, Pandini G, Scalia P, et al. Insulin receptor isoform A, a newly recognized, high-affinity insulin-like growth factor II receptor in fetal and cancer cells. *Mol Cell Biol*. 1999;19:3278–3288.
 23. Harrington SC, Weroha SJ, Reynolds C, Suman VJ, Lingle WL, Haluska P. Quantifying insulin receptor isoform expression in FFPE breast tumors. *Growth Horm IGF Res*. 2012;22:108–115.
 24. Chettouh H, Fartoux L, Aoudjehane L, et al. Mitogenic insulin receptor-A is overexpressed in human hepatocellular carcinoma due to EGFR-mediated dysregulation of RNA splicing factors. *Cancer Res*. 2013;73:3974–3986.
 25. Vella V, Pandini G, Sciacca L, et al. A novel autocrine loop involving IGF-II and the insulin receptor isoform-A stimulates growth of thyroid cancer. *J Clin Endocrinol Metab*. 2002;87:245–254.
 26. Gallagher EJ, Alikhani N, Tobin-Hess A, et al. Insulin receptor phosphorylation by endogenous insulin or the insulin analog AspB10 promotes mammary tumor growth independent of the IGF-I receptor. *Diabetes*. 2013;62:3553–3560.
 27. Benecke H, Flier JS, Moller DE. Alternatively spliced variants of the insulin receptor protein. Expression in normal and diabetic human tissues. *J Clin Invest*. 1992;89:2066–2070.
 28. Giudice LC, Dsupin BA, Jin IH, Vu TH, Hoffman AR. Differential expression of messenger ribonucleic acids encoding insulin-like growth factors and their receptors in human uterine endometrium and decidua. *J Clin Endocrinol Metab*. 1993;76:1115–1122.
 29. Paria BC, Ma W, Tan J, et al. Cellular and molecular responses of the uterus to embryo implantation can be elicited by locally applied growth factors. *Proc Natl Acad Sci USA*. 2001;98:1047–1052.
 30. Bruchim I, Sarfstein R, Werner H. The IGF hormonal network in endometrial cancer: functions, regulation, and targeting approaches. *Front Endocrinol (Lausanne)*. 2014;5:76.
 31. Kurman RJ, Kaminski PF, Norris HJ. The behavior of endometrial hyperplasia. A long-term study of “untreated” hyperplasia in 170 patients. *Obstet Gynecol Survey*. 1986;41:58–61.
 32. Wang CF, Zhang G, Zhao LJ, et al. Overexpression of the insulin receptor isoform A promotes endometrial carcinoma cell growth. *PLoS One*. 2013;8:e69001.
 33. Strowitzki T, Von Eye H, Kellerer M, Haring H. Tyrosine kinase activity of insulin-like growth factor I and insulin receptors in human endometrium during the menstrual cycle: cyclic variation of insulin receptor expression. *Int J Gynecol Obstet*. 1993;43:94–95.
 34. Mioni R, Mozzanega B, Granzotto M, et al. Insulin receptor and glucose transporters mRNA expression throughout the menstrual cycle in human endometrium: a physiological and cyclical condition of tissue insulin resistance. *Gynecol Endocrinol*. 2012;28:1014–1018.
 35. Flannery CA, Rowzee AM, Choe GH, et al. Development of a quantitative PCR assay for detection of human insulin-like growth factor receptor and insulin receptor isoforms. *Endocrinology*. 2016;157:1702–1708.
 36. Expert Panel on the Identification, Evaluation, and Treatment of Overweight and Obesity in Adults (US). Executive summary of the clinical guidelines on the identification, evaluation, and treatment of overweight and obesity in adults. 1998: National Institutes of Health, National Heart, Lung, and Blood Institute; Bethesda, Maryland.
 37. Noyes R, Hertig A, Rock J. Dating the endometrial biopsy. *Obstet Gynecol Survey*. 1950;5:561–564.
 38. Scully RE. *Histological Typing of Female Genital Tract Tumors (International Histological Classification of Tumors)*. New York, NY: Springer-Verlag; 1996.
 39. Pecorelli S. Revised FIGO staging for carcinoma of the vulva, cervix, and endometrium. *Int J Gynaecol Obstet*. 2009;105:103–104.
 40. Kliman HJ, Feinberg RF, Schwartz LB, Feinman MA, Lavi E, Meadough EL. A mucin-like glycoprotein identified by MAG (mouse ascites Golgi) antibodies. Menstrual cycle-dependent localization in human endometrium. *Am J Pathol*. 1995;146:166–181.
 41. Yang H, Zhou Y, Edelshain B, Schatz F, Lockwood CJ, Taylor HS. FKBP4 is regulated by HOXA10 during decidualization and in endometriosis. *Reproduction*. 2012;143:531–538.
 42. Arici A, Head JR, MacDonald PC, Casey ML. Regulation of interleukin-8 gene expression in human endometrial cells in culture. *Mol Cell Endocrinol*. 1993;94:195–204.
 43. Rowzee AM, Ludwig DL, Wood TL. Insulin-like growth factor type 1 receptor and insulin receptor isoform expression and signaling in mammary epithelial cells. *Endocrinology*. 2009;150:3611–3619.
 44. Ludwig H, Spornitz U. Microarchitecture of the human endometrium by scanning electron microscopy: menstrual desquamation and remodeling. *Ann NY Acad Sci*. 1991;622:28–46.
 45. Adesanya OO, Zhou J, Samathanam C, Powell-Braxton L, Bondy CA. Insulin-like growth factor 1 is required for G2 progression in the estradiol-induced mitotic cycle. *Proc Natl Acad Sci USA*. 1999;96:3287–3291.
 46. Klotz DM, Hewitt SC, Korach KS, Diaugustine RP. Activation of a uterine insulin-like growth factor I signaling pathway by clinical and environmental estrogens: requirement of estrogen receptor- α . *Endocrinology*. 2000;141:3430–3439.
 47. McCampbell AS, Broaddus RR, Loose DS, Davies PJ. Overexpression of the insulin-like growth factor I receptor and activation of the AKT pathway in hyperplastic endometrium. *Clin Cancer Res*. 2006;12:6373–6378.